Comparative study on zinc oxide nanocrystals synthesized by two precipitation methods

(Estudo comparativo em nanocristais de óxido de zinco sintetizados por dois métodos de precipitação)

M. R. Bodke[1], Y. Purushotham[2], B. N. Dole[1*]

[1]Advanced Materials Research Laboratory, Department of Physics, Dr. Babasaheb Ambedkar Marathwada University, Aurangabad-431 004, India

[2]Centre for Materials for Electronics Technology, IDA Phase III, Cherlapally, Hyderabad-500 051, India

[*]dolebn_phys@yahoo.in

Abstract

Zinc oxide nanocrystals were synthesized by two precipitation methods successfully. The nanocrystals prepared via method I (zinc acetate dihydrate precipitation with KOH) were smaller in crystallite size (~20 nm) as compared to method II (zinc nitrate hexahydrate precipitation with *N*,*N*-dimethylformamide, ~33 nm). FTIR technique was used to study chemical bonding; SEM and EDS were used to study morphology and chemical compositions. Number of concentric rings corresponding to diffraction peaks was higher in SAED pattern for ZnO nanocrystals synthesized by method I than II. Variation in the energy band gap as a function of particle size was determined using absorption spectra from UV-vis-NIR spectrophotometer. Redshift was observed in the energy band gap of sample prepared via method II. Particle size and the structure of the nanocrystals were analysed by transmission electron microscope (TEM). From TEM study, it was found that the average particle size of method I nanocrystals was smaller compared to method II nanocrystals. Magnetic study was carried out using VSM. Ferromagnetism like contribution was observed for the sample prepared by method II.
Keywords: ZnO nanocrystals, precipitation, redshift, crystallite size, energy band gap.

Resumo

Nanocristais de óxido de zinco foram sintetizados por dois métodos de precipitação. Os nanocristais preparados pelo método I (precipitação de acetato de zinco di-hidratado com KOH) foram menores em tamanho de cristalito (~20 nm) em comparação com o método II (precipitação de nitrato de zinco hexa-hidratado com N,N-dimetilformamida, ~33 nm). A técnica FTIR foi utilizada para estudar a ligação química; MEV e EDS foram utilizados para estudar a morfologia e composição química. O número de anéis concêntricos correspondentes aos picos de difração foi maior no padrão SAED para nanocristalinos de ZnO sintetizados pelo método I do que II. A variação da banda de energia proibida em função do tamanho de partícula foi determinada usando espectros de absorção UV-vis-NIR. Deslocamento para o vermelho foi observado na banda proibida da amostra preparada pelo método II. O tamanho de partícula e a estrutura dos nanocristais foram analisados por microscópio eletrônico de transmissão (MET). A partir do estudo de MET, verificou-se que o tamanho médio de partícula dos nanocristais do método I foi menor em comparação com os nanocristais do método II. O estudo magnético foi realizado com VSM. Contribuição do tipo ferromagnetismo foi observada para a amostra preparada pelo método II.
***Palavras-chave**: nanocristais de ZnO, precipitação, deslocamento para o vermelho, tamanho de cristalito, banda de energia proibida.*

INTRODUCTION

Zinc oxide has wide range of applications in varistors, pigment in paints and sunscreen for the prevention of sunburn due to its ability to absorb ultraviolet light. ZnO is most promising n-type oxide semiconductor with wide band gap of 3.37 eV at room temperature in bulk form, large exciton binding energy (60 meV), which is 2.4 times the effective thermal energy (25 meV), large saturation velocity ($3.2.10^7$ cm/s) and high break down voltage [1, 2]. ZnO crystallizes in three forms: (i) hexagonal, (ii) cubic zinc blende, and (iii) cubic rock salt. Hexagonal (wurtzite) is the main stable crystal structure of ZnO at room temperature [3]. ZnO nanostructures such as nanocrystals, nanorods, nanobelts, nanotubes and especially nanowires are attracting more and more attention due to their vital electronic, optical and magnetic properties as well as unique morphology for both interconnects and functional units in fabricating nanodevices [4-7]. Particularly, spintronics devices such as spin valve transistors, non-volatile memory, logic devices, ultrafast optical switches and optical isolators have stimulated great passions of many researchers for introducing room temperature ferromagnetism in nanostructured ZnO materials [8, 9].

Various synthesis methods have been used for the preparation of ZnO nanostructures such as vapour-liquid-

solid method, reaction vapour deposition, physical vapour deposition, pulsed laser deposition, thermal evaporation and chemical solution routes, like sol-gel, precipitation and hydrothermal methods [10, 11]. Among these synthesis routes, chemical solution routes are cost effective, convenient and have general advantages such as super uniformity and high yield of nanocrystals [12].

In the present study, ZnO nanocrystals were synthesized by two chemical precipitation routes, then compared the quality of the samples by XRD, optical properties, TEM, FTIR, EDS and VSM studies. Samples prepared by zinc acetate dihydrate precipitation with KOH carried higher quality than zinc nitrate hexahydrate precipitation with *N,N*-dimethylformamide. Results of such an investigation were elucidated qualitatively in this paper.

MATERIALS AND METHODS

Precipitation method I - zinc acetate dihydrate precipitation with KOH: the starting materials used for the synthesis of ZnO nanocrystals were zinc acetate dihydrate and KOH with 99% purity. The appropriate amounts of zinc acetate and potassium hydroxide were dissolved separately in 100 mL methanol and stirred at room temperature for 2 h. After fully dissolved, potassium hydroxide solution was added drop-wise with vigorous stirring resulting in a light sky-blue coloured precipitate. The precipitate was stirred again for 2 h to get homogeneous particle size. The precipitate was collected and washed several times by methanol followed by deionised water. Finally, ZnO nanocrystals were obtained after calcining the precursor at 450 °C for 12 h.

Precipitation method II - zinc nitrate hexahydrate precipitation with N,N-dimethylformamide: chemicals used in this method were zinc nitrate hexahydrate and *N,N*-dimethylformamide with 99% purity. Zinc nitrate hexahydrate of appropriate weight was dissolved in 50 mL *N,N*-dimethylformamide and stirred with a magnetic stirrer for 1 h at 40 °C. The solution was heated for 1 h at 150 °C for the formation of sol. The product was dried at 150 °C to form nanopowder and then ground for 15 min and calcined at 450 °C for 8 h to obtain ZnO nanocrystals.

Crystal structure of ZnO was determined by X-ray diffraction (XRD, Panalytical, PW-3710) with CuKα radiation (λ= 0.15406 nm). Scanning electron microscope (SEM, Jeol, JSM6360A) was used for the topographic study, and chemical compositional analysis of ZnO nanocrystals was carried out using an energy dispersive spectroscope (EDS). Fourier-transform infrared (FTIR, Jasco) spectra were recorded for chemical bonding. Magnetic studies of ZnO nanocrystals were outlined using vibrating sample magnetometer (VSM). Optical properties were investigated using UV-visible spectrometer (Jasco UV-VIS-NIR, V-670) in the range of 200 to 1000 nm to determine energy band gap.

RESULTS AND DISCUSSION

XRD study: XRD patterns of ZnO nanocrystals are depicted in Fig. 1. The crystal structure of the ZnO nanocrystals as synthesized by both routes belongs to hexagonal (wurtzite) structure, which is very close with standard JCPDS files (36-1451 and 01-071-6424) [13]. The diffraction peaks were in good agreement with the results reported in the literature [10, 12-14]. In this study, the diffraction peaks were slightly shifted to lower values of 2θ for ZnO sample prepared by preparation method II. Shifting of diffraction peaks shows increment in lattice parameters like lattice constants, volume of unit cell, X-ray density, APF and grain size.

By recording the full width at half maxima (FWHM) of these peaks, the grain size was determined using Debye-

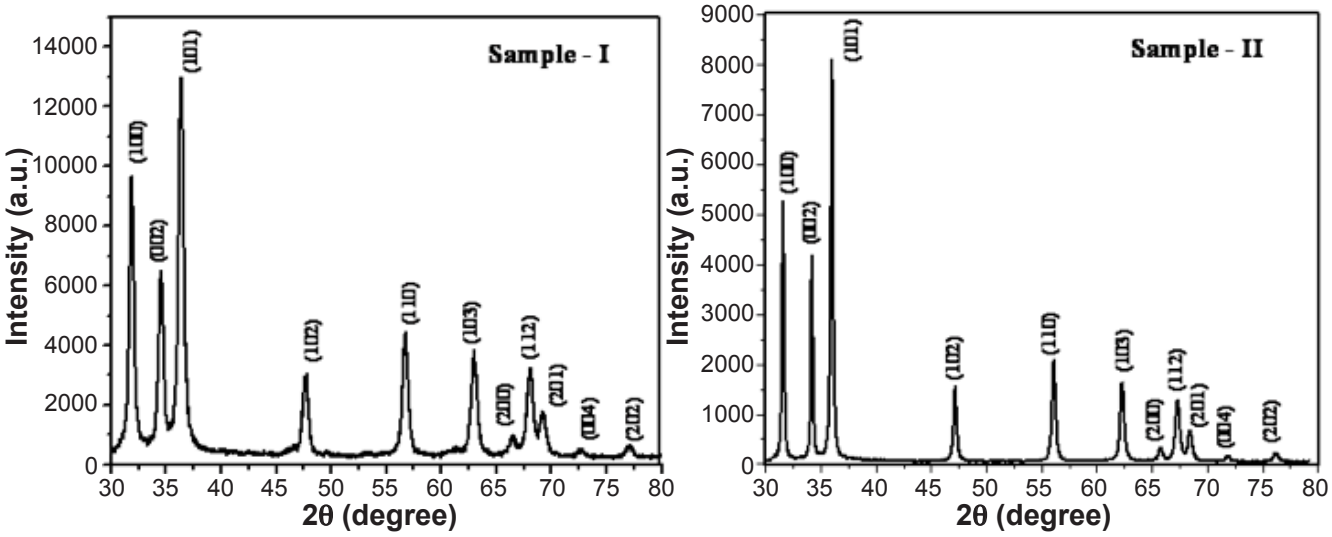

Figure 1: X-ray diffraction pattern for ZnO nanocrystals synthesized by two precipitation methods.
[Figura 1: Difratogramas de raios X para nanocristais de ZnO sintetizados por dois métodos de precipitação.]

Scherrer's formula:

$$D = \frac{K\lambda}{\beta\cos\theta} \qquad (A)$$

where K is the particle shape factor which depends on the shape of the particle and its value is 0.09 for hexagonal particles, λ is the wavelength of CuKα radiation (0.15406 nm), β is the full width at half maximum of the selected diffraction peak corresponding to (110) plane and θ is the Bragg angle obtained from 2θ corresponding to the same plane. The grain size, lattice parameters, volume cell, X-ray density and atomic packing fraction (APF) of the samples were determined from XRD data and listed in Table I. The lattice constants a and c, volume of unit cell, and grain size of the ZnO nanocrystals were higher for method II than method I; whereas, X-ray density and atomic packing fraction (APF) values were higher for ZnO synthesized by method I.

Chemical bonding study: FTIR measurements were performed in the wavenumber range 4000 to 400 cm^{-1} using KBr method to confirm the formation of crystalline ZnO nanoparticles synthesized by precipitation methods I and II as shown in Fig. 2 and to identify absorbed species into the crystal surface. In FTIR absorption spectra of ZnO nanocrystals synthesized by precipitation route I, broad band was observed around 3380 cm^{-1} which appears typically due to stretching and bonding modes of hydroxyl (O-H) group of H_2O [15]. The additional weak band was detected around 2116 cm^{-1}. The band arising from the absorption of atmospheric CO_2 on the metallic cations at 1585 cm^{-1} [16] and shoulder with asymmetric stretching was detected at around 1010 cm^{-1}. ZnO absorption stretching was observed at around 887 cm^{-1}, and the band at 605 cm^{-1} is the stretching mode of ZnO [17]. For the sample synthesized by method II, broad band occurred around 3408 cm^{-1} which exists due to stretching and bonding modes of hydroxyl (O-H) group of H_2O. The additional weak band was around 2251 and 2360 cm^{-1}. Band arising from the absorption of atmospheric CO_2 on the metallic cations was at 1482 cm^{-1} and shoulder with asymmetric stretching was detected at around 1222 cm^{-1}. ZnO absorption stretching was observed at around 938 cm^{-1}, and the band at around 613 cm^{-1} is the stretching mode of ZnO.

Surface morphology: SEM images of ZnO nanocrystals are shown in Fig. 3. The image of the ZnO nano crystals

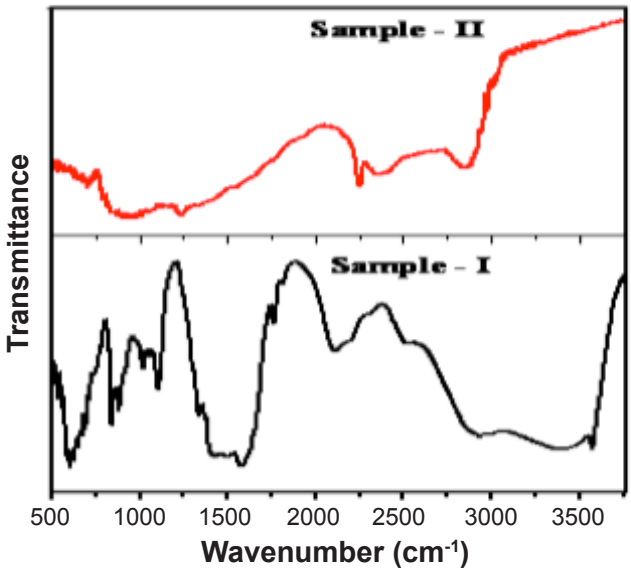

Figure 2: FTIR spectra of ZnO nanocrystals.
[Figura 2: Espectros de FTIR de nanocristais de ZnO.]

prepared by method I shows single morphology like flowery structure and the samples prepared by method II are transparent and crystalline form without aggregation of the particles. This may be due to larger grain size of the particle than that of the particles synthesized by method I. The images show that the synthesized nanoparticles are homogenous, uniformly distributed over the surface. Kumar *et al.* [18] reported different morphologies obtained for the ZnO samples calcined at three different temperatures.

Compositional analysis: EDS spectra of the ZnO nanocrystals are also shown in Fig. 3. Zn and O peaks are observed with no formation of secondary phases. In the sample prepared by method I, a K peak was detected, which may be due to using of KOH during the synthesis, and a C peak was observed in the EDS spectrum of ZnO nanocrystal sample by method II, which may be due to more exposed area of carbon sticker used for the characterization. Platinum peaks were detected in both spectra, which could be due to the platinum coating made at the time of characterization. Kumar *et al.* [18] also reported that EDS study of ZnO samples by method II had pure ZnO phases. From EDS spectra, it was revealed that ZnO nanoparticles synthesized by method II

Table I - Lattice parameters, X-ray density, unit cell volume, grain size and atomic packing fraction (APF) values of ZnO nanocrystals.
[Tabela I - Parâmetros de rede, densidade de raios X, volume de célula unitária, tamanho de grão e fração de empacotamento atômico (APF) dos nanocristais de ZnO.]

Sample code / synthesis route	a (Å)	c (Å)	X-ray density (g/cm^3)	Volume of unit cell ($Å^3$)	Grain size (nm)	APF (%)
Sample I / precipitation method I	3.241	5.189	5.728	47.21	19.8	75.5
Sample II / precipitation method II	3.249	5.261	5.623	48.09	33.3	74.7

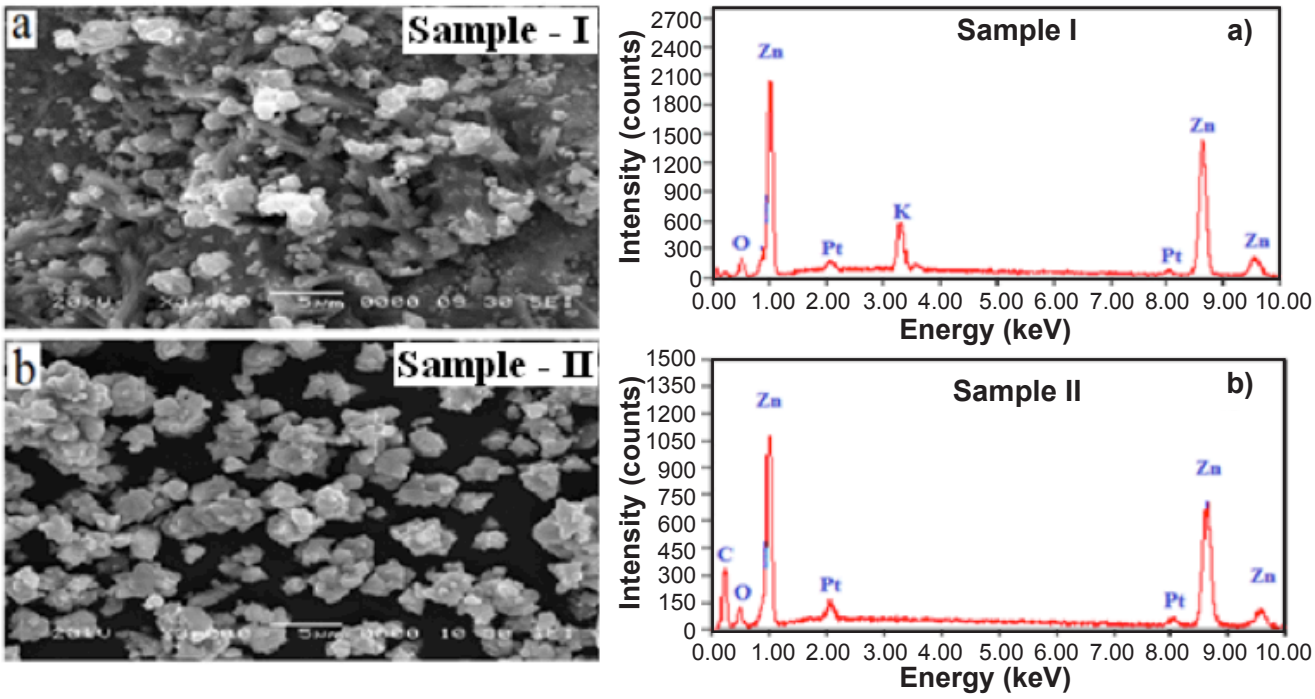

Figure 3: SEM micrographs (left) and EDS spectra (right) of ZnO nanocrystals.
[Figura 3: Micrografias obtidas por microscopia eletrônica de varredura (esquerda) e espectros de EDS (direita) de nanocristais de ZnO.]

were highly pure, more than that from method I.

TEM study: Fig. 4 shows TEM (transmission electron microscopy) images and SAED (selected area electron diffraction) patterns of ZnO nanocrystals. Bagabas *et al*. [19] reported that clear morphology was observed for the calcined samples and not in the case of uncalcined samples. But, it is clearly observed from the images that the particles have hexagonal (wurtzite) structure and average particle size of the nanocrystals synthesized by method I was smaller than the nanocrystals by method II. SAED patterns for ZnO nanocrystals prepared by precipitation methods I and II are given in the inset of Fig. 4. Mote *et al*. [20] and Prabhu *et al*. [14] reported that SAED pattern was not clear with the concentric rings. But in the present investigation, SAED pattern for ZnO nanocrystals synthesized by method I consisted of eleven sharp and bright concentric rings, which correspond to (100), (002), (101), (102), (110), (103), (200), (112), (201), (004) and (202) diffraction planes of the ZnO in hexagonal structure and the SAED pattern of ZnO nanocrystals prepared via method II consisted of six concentric sharp rings, which corresponded to (100), (002), (101), (102), (110), (103) and (112) planes of the ZnO in hexagonal structure.

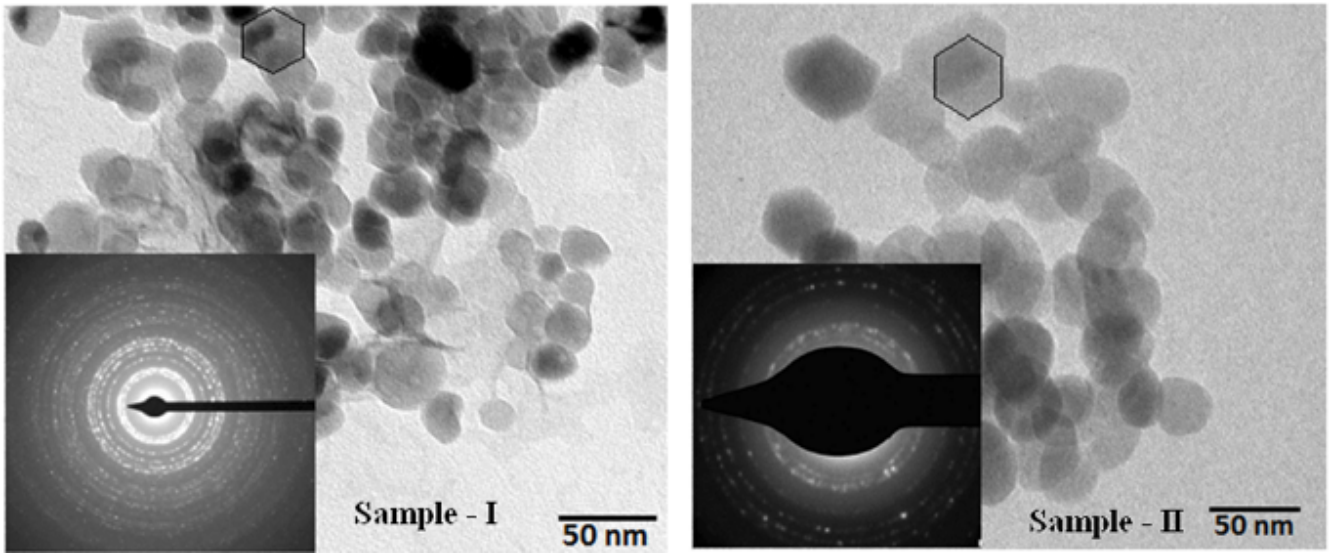

Figure 4: TEM images with SAED patterns for ZnO nanocrystals.
[Figura 4: Micrografias obtidas por microscopia eletrônica de transmissão com padrões SAED para nanocristais de ZnO.]

Energy band gap estimation: the UV-visible optical absorption spectra of the ZnO nanoparticles were carried out in the range of 200 to 1000 nm and are shown in Fig. 5a. Absorption band-edges observed for the nanoparticles of ZnO synthesized by both methods were around 363 and 361 nm, which is slightly higher than that of the observed value for pure ZnO nanorods (355 nm) in [21] and less than the reported value (366 nm) in [22]. Energy band gap of the sample was estimated by following Tauc's equation [23]:

$$\alpha h\nu = A(h\nu - Eg)^n \quad (B)$$

where α is the absorption coefficient, hν is the photon energy, A is the constant, E_g is the energy band gap of the sample. The value of n is 1/2 or 2 depending upon whether the transition from valence band to conduction band is direct or indirect. The value is 1/2 in case of direct transition and 2 in case of indirect transition. Since ZnO has a direct band structure, the value of n is 1/2 in this case. So, Eq. B becomes:

$$(\alpha h\nu)^2 = B(h\nu - Eg) \quad (C)$$

where B is a constant related effective mass of charge carriers associated with valence and conduction bands. Intersection of the slope of $(\alpha h\nu)^2$ vs hν curve provides band gap energy of the samples. The energy band gap was calculated from the absorption plot of energy (E=hν) versus $(\alpha h\nu)^2$ and is shown in Fig. 5b. In the present work, band gaps of ZnO samples synthesized by precipitation methods I and II were 3.08 and 3.04 eV, respectively, which were less than the reported values [22]. Also, they confirmed that Eg is higher for ZnO nanocrystals synthesized by method I than II.

Magnetic studies: Fig. 6 shows the M-H plots with field strength up to 1 T for ZnO nanocrystals synthesized by precipitation methods I and II. Magnetic study revealed that

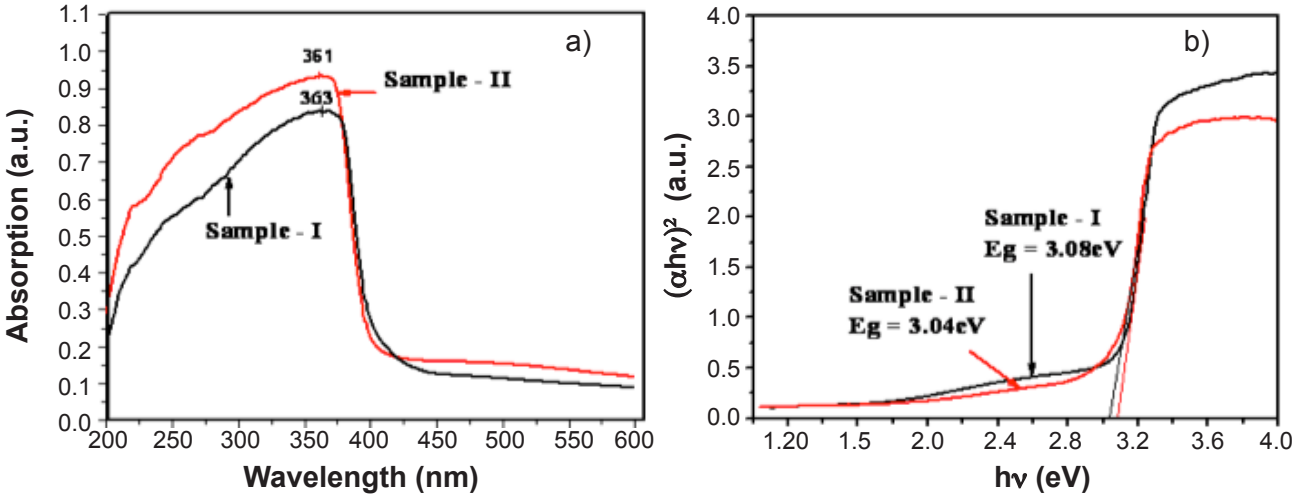

Figure 5: Absorption spectra (a) and Tauc plots (b) for ZnO nanocrystals.
[Figura 5: Espectros de absorção (a) e gráfico de Tauc (b) para nanocristais de ZnO.]

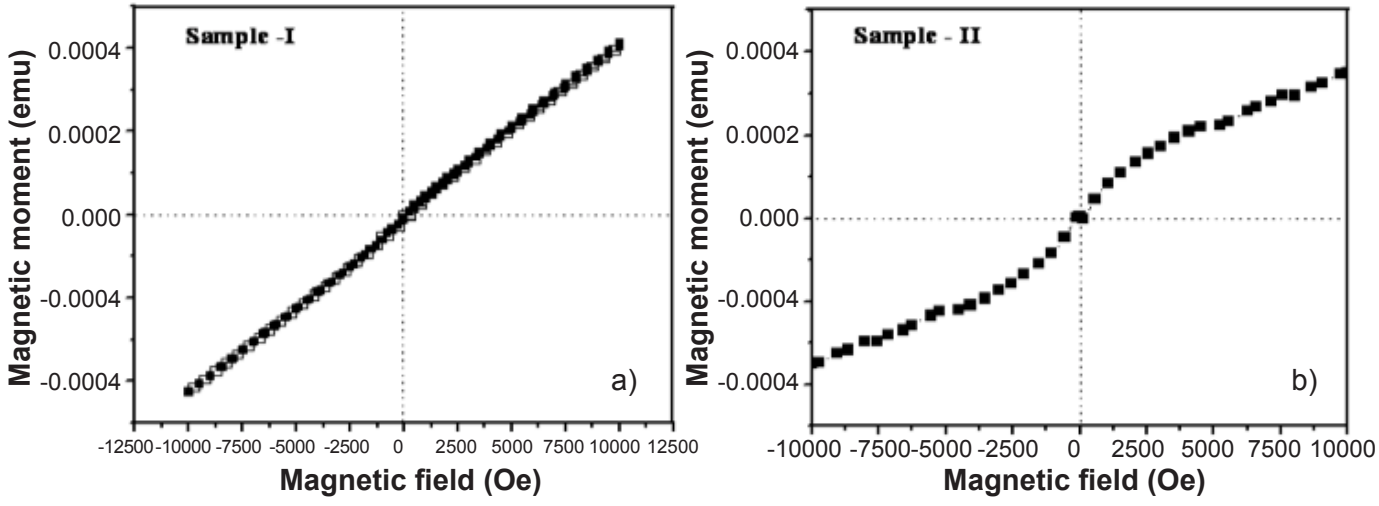

Figure 6: M-H plots of ZnO nanocrystals.
[Figura 6: Gráficos M-H de nanocristais de ZnO.]

nanocrystals synthesized by method I showed diamagnetism similar to bulk ZnO. Garcia *et al*. [24] reported ferromagnetic-like contribution for the AMINE- and THIOL-capping agents. But in our study, without using any such capping agents, sample synthesized by method II had ferromagnetic like contribution at room temperature. It implies that magnetic property can be varied from one preparation route to another.

CONCLUSIONS

Zinc oxide nanocrystals were synthesized by precipitation methods I (zinc acetate dihydrate precipitation with KOH) and II (zinc nitrate hexahydrate precipitation with *N*,*N*-dimethylformamide). Hexagonal wurtzite structure was observed from XRD and confirmed by TEM. ZnO nanocrystals synthesized by precipitation method I were found smaller than the nanocrystals synthesized by method II. It was found that CO_2 modes were present in the FTIR spectra, may be due to atmospheric CO_2 in the samples. The powder prepared by precipitation method I had a potassium contamination which was responsible by the change in the particle growth and CO_2 adsorption. Presence of foreign cations during the nanopowder preparation can change the particle growth and the surface properties due to segregation. In this work, the K^+ has different ionic radius, charge and electronegativity than the host that can promote the surface segregation, and probably change in the surface composition which stabilize the surface and the particle growth. Whereas, in method II, the dimethylformamide is a strong base (pK_b= 3.99) that promoted the precipitation by pH change. However, some organic contamination could be involved in the crystallization as shown in the FTIR analysis. Atomic packing fraction was well matched with the standard data. It was confirmed from TEM that the sample prepared by method II was highly crystalline than the nanocrystals synthesized by method I. Number of concentric rings corresponding to the diffraction peaks was higher in the SAED pattern for ZnO nanocrystals synthesized by method I than II. Energy band gap of ZnO nanocrystals synthesized by method I was higher than the nanocrystals prepared by method II. ZnO nanocrystals synthesized by method II showed at room temperature small signature of ferromagnetism. Finally, it was concluded that the sample synthesized by precipitation method I gave better results than method II.

REFERENCES

[1] X. Zi-Qiang, D. Hong, L. Yan, C. Hang, Mat. Sci. Semi. Proc. **9** (2006) 132.
[2] W. Jun, Y. Yantang J. Mat. Lett. **62** (2008) 1899.
[3] D.P. Norton, M. Ivill, Y. Li, Y.W. Kwon, J.M. Erie, H.S. Kim, K. Ip, S.J. Pearton, Y.N. Heo, S. Kim, B.S. Kang, F. Ren, A.F. Hebard, J. Kelly, Thin Solid Films **496** (2006) 160.
[4] D. Wang, C. Song, J. Phys. Chem. B **109** (2005) 12697.
[5] P.X. Gao, Y. Ding, W. Mai, W.L. Hughes, C. Lao, Z.L. Wang, Science **309** (2005) 1700.
[6] H. Yu, Z. Zhang, M. Han, X. Hao, F. Zhu, J. Am. Chem. Soc. **127** (2005) 2378.
[7] C. Lu, L. Qi, J. Yang, L. Tang, D. Zhang, J. Ma, Chem. Commun. **33** (2006) 3551.
[8] J.J. Liu, K. Wang, M.H. Yu, W.L. Zhou, J. Appl. Phys. **102** (2007) 024301.
[9] J. Cui, Q. Zeng, U.J. Gibson, J. Appl. Phys. **99** (2006) 08M113.
[10] U. Manzoor, Md. Islam, L. Tabassam, S.U. Rahman, Physica E **41** (2009) 1669.
[11] R. Bhargava, P.K. Sharma, S. Kumar, A.C. Pandey, N. Kumar, J. Sol. State Chem. **183** (2010) 1400.
[12] Y. Hu, H. J. Chen, J. Nanopart. Res. **10** (2008) 401.
[13] D.K. Bhat, Nanoscale Res. Lett. **3** (2008) 31.
[14] Y.T. Prabhu, K.V. Rao, V.S.S. Kumar, B.S. Kumari, World J. Nano Sci. Eng. **4** (2014) 21.
[15] S. Maensiri, P. Laokul, V. Promarak, J. Cryst. Growth **289** (2006) 102.
[16] J.W. Drazin, R.H.R. Castro, J. Am. Ceram. Soc. **99** (2016) 1105.
[17] K. Nakamoto, *Infrared spectra of inorganic and coordination compounds*, Wiley, New York (1997).
[18] S.S. Kumar, P. Venkateswarlu, V.R. Rao, G.N. Rao, Int. Nano Lett. **3** (2013) 30.
[19] A. Bagabas, A. Alshammari, M.F.A. Aboud, H. Kosslick, Nanoscale Res. Lett. **8** (2013) 516.
[20] V.D. Mote, Y. Purushotham, B.N. Dole, J. Theor. Appl. Phys. **6** (2012) 6.
[21] M.K. Gupta, N. Sinha, B. Kumar, J. Appl. Phys. **112** (2012) 014303.
[22] R.S. Kumar, R. Sathyamoorthy, P. Sudhagar, P. Matheswaran, C.P. Hrudhya, Y.S. Kang, Physica E **43** (2011) 1166.
[23] A.B. Kashyout, M. Soliman, M. El Gamal, M. Fathy, Mat. Chem. Phys. **90** (2005) 230.
[24] M.A. Garcia, J.M. Merino, E.F. Pinel, A. Quesada, J. de la Venta, M.L.R. Gonzalez, G.R. Castro, P. Crespo, J. Llopis, J.M. Gonzalez-Calbet, A. Hernando, Nano Lett. **7** (2007) 1489.
(Rec. 15/12/2016, Rev. 24/03/2017, 25/04/2017, Ac. 21/06/2017)

(cc) BY-NC